Plasticity of the MFS1 promotor is not the only driver of Multidrug resistance in Zymoseptoria tritici

Simon Patry-Leclaire, Elza Neau, Anaïs Pitarch, Anne-Sophie Walker, Sabine Fillinger

Plasticity of the MFS1 promotor is not the only driver of Multidrug resistance in Zymoseptoria tritici

Authors : Simon Patry-Leclaire, Elza Neau, Anaïs Pitarch, Anne-Sophie Walker, and Sabine Fillinger

Background

Multidrug resistance has been identified in the fungal pathogen responsible for Septoria leaf blotch, *Zymoseptoria tritici*, since 2011. It has been linked to the overexpression of the gene encoding the MFS1 transporter due to inserts in the promoter region of *MFS1* (P_{MFS1}), namely types I-III. Recently, two new inserts were discovered in P_{MFS1} that were not linked to MDR, interrogating about whether P_{MFS1} inserts are the only drivers of MDR in *Z. tritici*.

The goal of our study was to gain a more complete view of MDR in *Z. tritici* by examining the genotypic diversity associated with the MDR phenotype in a large sample of the modern population.

Results

We isolated 384 potential MDR strains between 2020 and 2021 in northern Europe for P_{MFS1} genotype and MDR assessment. We discovered six new inserts in P_{MFS1}, bringing the total count to 13 including one insertion-deletion in the 5' UTR region. Of these, 11 display similarities with transposable elements, and 3 are not linked to MDR. Some field strains were significantly more resistant than their respective reference of the same P_{MFS1} genotype and some strains without insert displayed MDR phenotype.

Conclusion

We described the landscape of the MDR in modern *Z. tritici* population and postulate that P_{MFS1} is a hot-spot for insertions involving transposition events. Our study shows that MDR cannot be solely explained by inserts found in P_{MFS1}, and that additional mechanisms might be at work.

Introduction 2023

The ascomycete *Zymoseptoria tritici* causes Septoria leaf blotch in wheat, leading to significant yield losses worldwide (Fones & Gurr, 2015). This widespread pathogen affects both bread wheat and durum wheat, and is the most damageable wheat pathogen in Europe particularly in temperate climates (Klink et al., 2021; Torriani et al., 2015).

Besides the use of resistant or tolerant wheat varieties, the most commonly used control method to decrease the impact of *Z. tritici* in the field, is the application of fungicides. Several unisite fungicides with different modes of action are recommended for use in the field, targeting various but specific metabolic enzymes. They include succinate dehydrogenase inhibitors (SDHIs), 14-demethylation inhibitors (DMIs), and since very recently the quinone inside inhibitor (QiI) fenpicoxamid, while quinone outside inhibitors (QoI) have lost efficacy against STB due to generalized resistance (Garnault et al., 2019). Inhibitors targeting multiple cellular targets such as sulfur or folpet may also be applied, especially as preventive, first treatment, eventually in association with a unisite fungicide .

However, *Z. tritici* has developed resistance against single-site fungicides (reviewed by Lucas et al., 2015). These resistances can either occur through target-site modifications generally inducing alterations in the fungicide binding site or through the overexpression of the fungicide target. This is the case for DMI resistance, where target mutations in *CYP51* have steadily increased since their introduction in the 1970s, with the frequency of these mutations rising in field populations in Europe (Garnault et al., 2019; Huf et al., 2018).

In addition to target-site resistance, non-target site resistance may occur through several processes with variable effects on fungicide efficacy, most of which are still misunderstood in fungal plant pathogens (Hu & Chen, 2021). Probably, the most prominent mechanism is increased efflux leading to multidrug resistance (MDR), conferring unspecific resistance to unisite fungicides. MDR has been revealed in some plant pathogenic fungi so far (e.g., *Botrytis cinerea, Oculimacula spp*., *Penicillum digitatum* & *P. expansum, Clarireedia*

homoeocarpa (formerly *Sclerotinia homoeocarpa*), and *Z. tritici* (Kretschmer et al., 2009; Leroux et al., 2013; Sang & Hulvey, 2018; Sun et al., 2013)).

In *Z. tritici* MDR confers moderate resistance to SDHIs, QoIs, and DMIs (Leroux & Walker, 2011; Omrane et al., 2015), but combined to target-site resistance MDR leads to particularly high resistance factors as in the case of DMI resistance. *In vitro*, the selection of multidrug resistant strains of *Z. tritici* was favored by alternation or mixture of fungicides (Ballu et al., 2021).

Multidrug resistance has been characterized in some plant pathogenic fungi: in *Botrytis cinerea*, MDR is linked to the overexpression of the ABC transporter gene *BcAtrB* caused by a gain-of-function mutation in the transcription factor *BcMrr1*. MDR is also associated with the insertion of a retrotransposon in the promoter region of the gene encoding an MFS transporter (*BcMfsM2*) (Kretschmer et al., 2009). In *Clarireedia homoeocarpa* multidrug resistance is linked to the joint overexpression of three CYP450 encoding genes and two ABC transporter encoding genes (Sang & Hulvey, 2018). The joint overexpression of these genes involved in phase I and III detoxification pathways is due to a gain-of-function mutation in the transcription factor (ShXDR1). The heterologous expression of this transcription factor SHXDR1 confers MDR to transformed *B. cinerea* strains.

Multidrug resistance (MDR) in *Z. tritici* has been associated with drug efflux as well (Omrane et al. 2015). This drug efflux mechanism is regulated by the expression of *MFS1*, a gene encoding an MFS transporter that enhances the efflux of DMIs, QoIs, and SDHIs outside the cytoplasm (Fouché et al., 2022, Omrane et al. 2015, 2017). It has been observed that *MFS1*

overexpression is due to the insertion of a 519 bp element in its promoter region, which was the first insert identified and characterized in relation to the MDR phenotype in this pathogen. Subsequently, type II and III inserts were detected in the *MFS1* promoter (P_{MFS1}; Omrane et al., 2017). From 2008 to 2017, the landscape of MDR strains was predominantly dominated by the genotype harboring the type I allele (75%) (Garnault et al. 2019). In 2018 and 2021 respectively, new inserts (furtheron named type IV and V inserts) were found but were not associated with the MDR phenotype (Lavrukaitė et al. 2023; Mäe et al. 2020). A population survey using PCR around the previously identified *MFS1* promoter inserts revealed an unsuspected P_{MFS1} allele diversity (at least 8 different amplicon sizes; Huf et al, 2020).

Concerning the origins of these insertions, the type I insert corresponds to an LTR transposon (Omrane et al., 2017), and also type IV was classified as potential transposon (Maë et al., 2020), suggesting frequent transposition events in the promoter region of *MFS1*. Transposable elements (TEs) play a significant role in the evolution and adaptation of plant pathogens (Möller & Stukenbrock, 2017; Oggenfuss et al, 2023; Singh et al., 2021). These mobile genetic elements are ubiquitous in the genome of *Z. tritici* (Lorrain et al. 2021) with a proportion in the genome between 14 to 21.5 % (Badet et al., 2020). They are found in higher density within the core chromosomes of the genome, and the analysis of their insertion frequencies in around twenty genomes suggests the existence of TE burst centers (Oggenfuss et al. 2023).

In the field, multidrug resistance (MDR) detection is commonly achieved through genotyping using endpoint PCR (Huf et al., 2018; Lavrukaitė et al., 2023; Mäe et al., 2020; Omrane et al., 2017). However, the reliability of a single PCR method in accurately identifying MDR without the occurrence of false negatives or false positives is of critical concern. Therefore, the objective of this study was to evaluate the P_{MFS1} genotypic diversity and the MDR phenotypic diversity of *Zymoseptoria tritici* in Europe during the period of 2020-2021, with the aim of establishing the correspondence between genotype and MDR phenotype. Our study revealed unprecedented promoter diversity at the *MFS1* locus; albeit not all inserts lead to MDR. Interestingly, some strains with known P_{MFS1} genotypes but higher MDR levels hint to additional mechanisms involved in multi-drug resistance in *Z. tritici*.

Results

Large-scale sampling of *Z tritici* MDR isolates

Isolates of *Z. tritici* were gathered in Northern Europe in 2020 and 2021. Most of the populations used for this study were collected from fields in France and provided by the ”Performance network” (*Garnault et al. 2019*). To isolate potential MDR strains we inoculated spore-solutions from wheat leaves on Petri dishes containing the medical fungicides tolnaftate or terbinafine at their respective discriminating concentrations (adapted after Leroux & Walker, 2011; Experimental procedures). Both molecules are inhibitors of squalene epoxidase (*Ryder et al. 1992*). By this way, we obtained 282 potential MDR isolates from France; other isolates were provided by our collaborators, namely 28 from Germany, 26 from the United Kingdom, 23 from Ireland, 12 from Lithuania, six from Belgium, two from Estonia and one from Denmark (Table S1). It has to be highlighted that only MDR isolates from France were selected on terbinafine or tolnaftate, while those from other countries had been

selected for their particular *MFS1* gene promoter (P_{MFS1}) genotypes or their resistance phenotypes to terbinafine or tolnaftate.

We then genotyped the promoter of the *MFS1* gene (P_{MFS1}) of all 384 isolates by PCR as previously described using the primer pair 2F-4R *(Omrane et al, 2017*). The results show a higher diversity than expected. Namely, we found strains with previously unidentified inserts, but also potential MDR strains without inserts. The most frequent P_{MFS1} alleles were of type I and type II (Table S1). Roughly 12% of the strains had no insert (n=46); the P_{MFS1} type III allele was found less frequently (<6%) in addition to other genotypes either with previously unknown inserts (see below) or one isolate whose promoter sequence could not be amplified and sequenced.

Table 1: Summary of inserts detected in P_{MFS1} in previous and the present study. Inserts are listed according to their localization relative to the start codon. Insert numbering is chronological according to time of discovery.

position relative to start codon (bp)	**Insert size (bp)**	**Insert name**	**Reference**
-108	Insertion/deletion (164/678)	Indel VIII	This study
-197/194	1884	type IV	Mäe and al., 2020
-203	150	type III	Omrane and al., 2017
-215	360	type VI	This study

-344	1940	type V	Lavrukaite et al., 2022 / This study
-397	519	type I	Omrane et al., 2017
-468	369	type IIA	Omrane and al., 2017
-468	338	type IIB	Omrane and al., 2017
-468	267	IIC	This study
-468	339	IID	This study
-468	298	IIE	This study
-468	328	IIF	This study
-468	327	type VII	This study

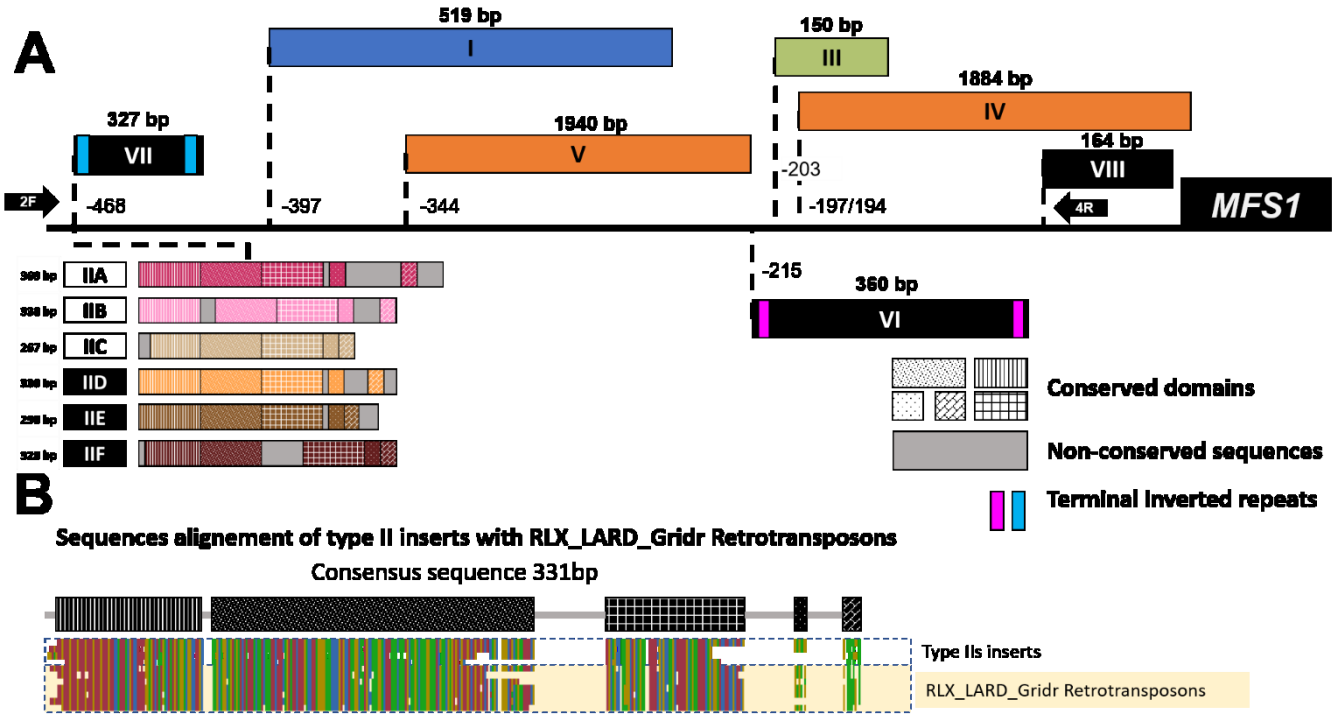

Figure 1 ***Molecular structure of MFS1 promoter genotypes****. A/ Insertion sites, sizes, and representation of the different inserts; those discovered in this study depicted in black. Terminal*

inverted repeats are highlighted in fuchsia and turquoise. Additionally, conserved domains in type 2 inserts are shown as filled patterns, while non-conserved domains are represented in gray. B/ Alignment of consensus sequences of type II inserts with the end of retrotransposons RLX_LARD_ridr found in the genome of Z. tritici, highlighted in yellow. Bases in type II insert and retrotransposon alignments are color-coded : A in green, T in red, G in yellow, and C in blue, with mismatches between the consensus sequence and the aligned sequence indicated by the absence of a base.

New inserts detected in P_{MFS1}

Table 1 summarizes the current knowledge of *MFS1* promoter inserts from previous (Lavrukaitė et al., 2023; Mäe et al., 2020; Omrane et al., 2017) and the present study. We have arbitrarily numbered all known and sequenced inserts chronologically according to the date of their discovery. Five new inserts were identified at the same insertion locus (at position -468 relative to the *MFS1* start codon) as the previously reported type II inserts (IIA and IIB). Among the newly detected inserts, four (IIC, IID, IIE, and IIF) share conserved domains with the previously described type II inserts, ranging in size from 267 bp to 339 bp. The fifth insert, however, does not exhibit any similarity with the type II inserts and was therefore referred to as the type VII insert. Further analysis using the reannotated genome of *Z. tritici* (Lapalu 2023) revealed that the conserved domains (totaling five) of type II inserts show similarities with retrotransposons from the RLX_Lard_Gridr family (Figure 1B).

Additionally, with the new annotated genome, we found that the entire type III insert aligns with the end of annotated transposable elements located on chromosomes 1, 8, 10, and 12. These transposable elements vary in size from 625 bp to 7060 bp.

Another new insert, measuring 360 bp, was identified in P_{MFS1} at a novel insertion site (-215 from the start codon of *MFS1*) and was designated as the type VI insert. Additionally, a new insertion was detected in a French isolate. Initially, this insertion could not be detected using the routine 2F-4R primer pair, as it failed to yield an amplification product. However, by designing new primers located relatively up- and downstream from the 2F-4R primer pair (see Experimental Procedures), we were able to successfully amplify the promoter region. Sequencing revealed a deletion of 678 bp between nucleotides 786 and 108 bp upstream of the start codon. Alongside this deletion, an insertion of 164 bp was detected. We have named this insertion/deletion “indel VIII”.

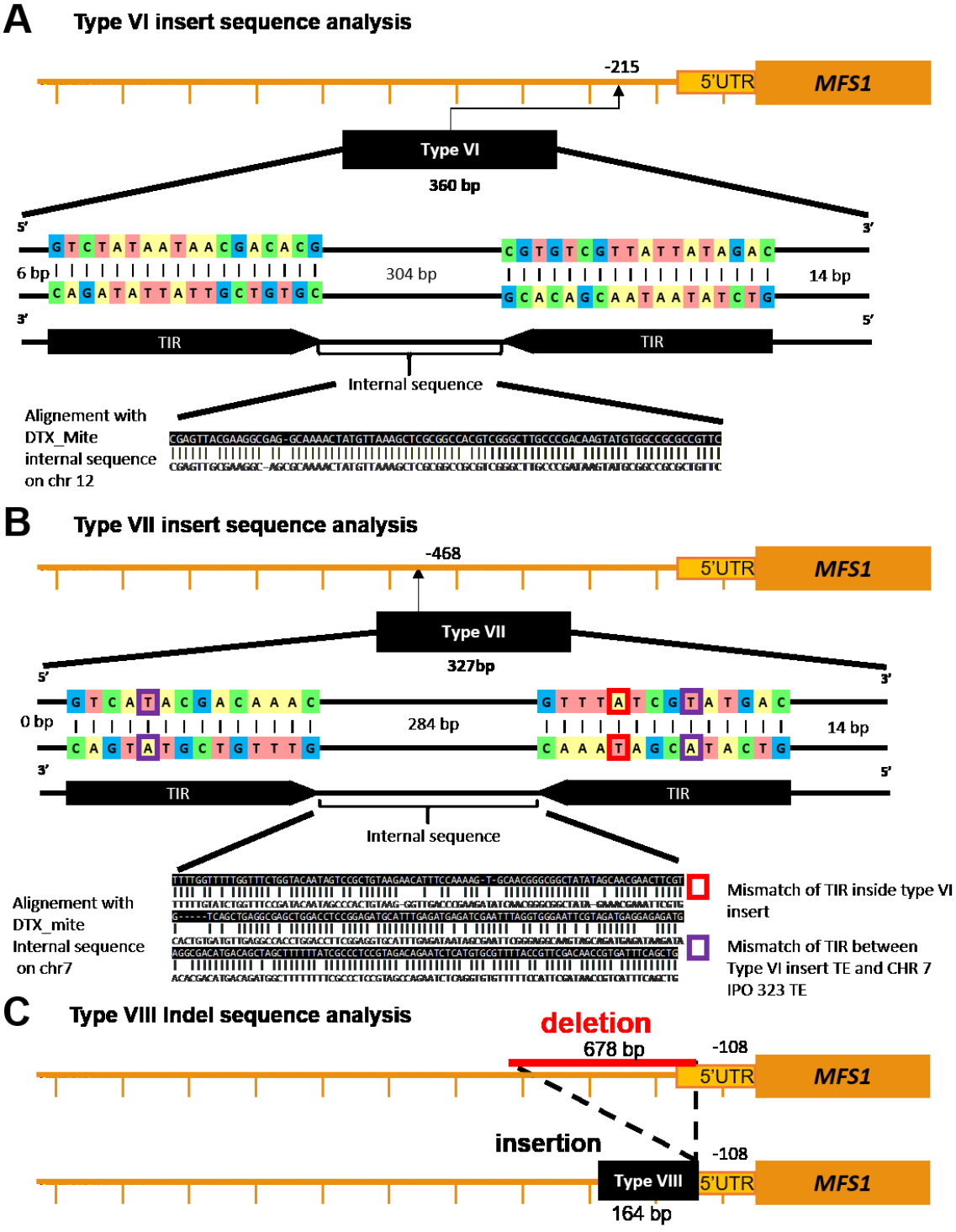

Figure 2 : Molecular structure of the new P_{MFS1} inserts found in Z. tritici field isolates. Insertion site position relative to the start-codon and length of the inserts are indicated. Coloured bases represent terminated inverted repeat (TIR) pairs identified in insert types VI and VII. Alignments with known sequences from other genomic regions are displayed.

Both new inserts, type VI and VII, correspond to miniature inverted repeat transposable elements (MITEs) (*Badet et al. 2021*). They contain short conserved terminal inverted repeats (TIRs) of 18 bp for the type VI insert and 14 bp for the type VII insert, respectively. Aligning the type VI insert sequence on the *Z. tritici* reference genome (Goodwin et al., 2011 (Lapalu et al., 2023) shows 91.57% identity to 89 bp of the internal sequence of another DTX MITE of a total size of 402 bp localized on chromosome 12 (Fig. 2). From the internal sequences of the type VII insert, 256 base pairs align with the internal sequences of a 323-base pair long DTX_MITE with 76.17% identity. This DTX_MITE transposable element was identified upstream of a gene encoding a putative unnamed protein on chromosome 7 (~~annotated with Ingenannot~~ Lapalu et al., 2023). For the Indel VIII the 678 bp deletion affects a portion of the 5'UTR region, removing 58 bp out of 166 bp. The inserted sequence does not show similarity to a known transposable element nor typical TE structure (according to most recent annotation of *Z. tritici* genomes).

Resistance profiles vary among P_{MFS1} genotypes

To validate terbinafine resistance and to establish MDR resistance profiles we tested 333 isolates from our 2020-2021 collection of *Z. tritici* through a droplet growth test on terbinafine and tolnaftate on a range of concentrations. We classified the resistance profiles into three categories, from low to high resistance according to the growth patterns observed (Table S.1, Figure S3)

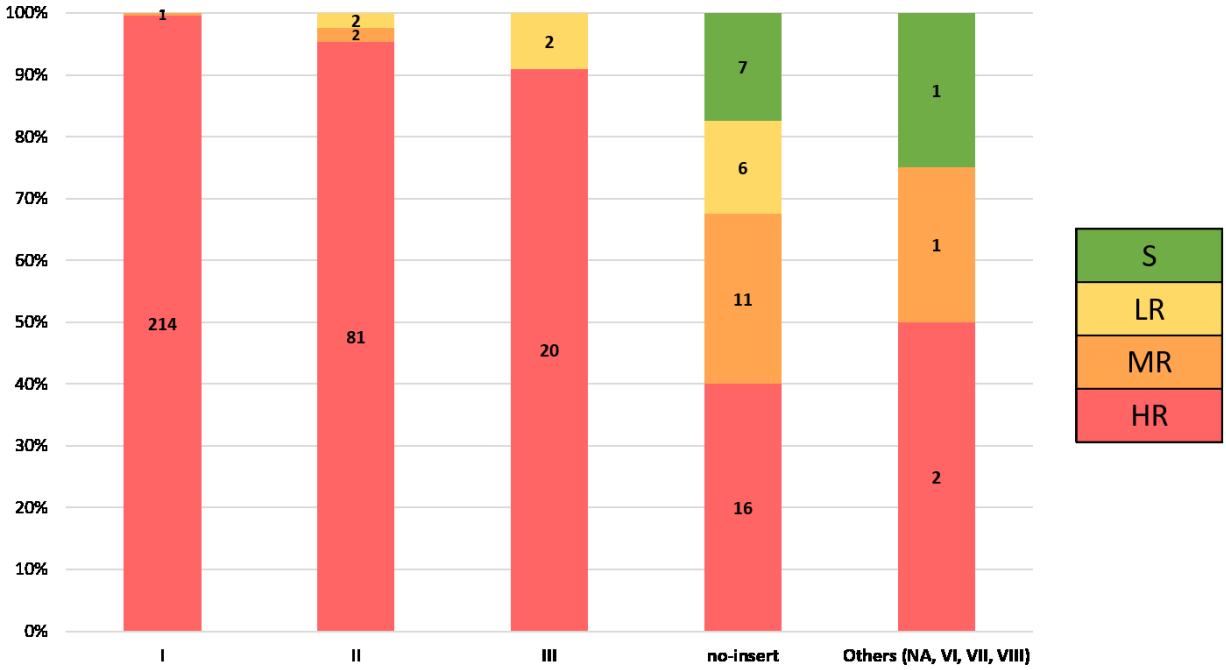

Figure S3 Distribution of terbinafine resistance among Z. tritici isolates of different P_{MFS1} genotypes. The MDR phenotypes are indicated as follows: HR, High Resistance; MR, Medium Resistance; LR, Low Resistance to terbinafine; S, Sensitive

Looking at the resistance profiles (Figure S3) isolates with the P_{MFS1}-type I allele had the most homogeneous resistance to terbinafine. 214 out of 215 tested strains displayed high resistance to terbinafine. On the other hand, isolates with the P_{MFS1}-no insert allele (n=40) were those with the most heterogenous resistance profiles ranging from sensitive (S) to highly resistant (HR).

Based on these results the original collection of 380 strains was downsized for further analysis. Among the isolates carrying the type II insert, 75 isolates were selected, among isolates carrying the type III insert, 14 isolates inserts were selected. Among the isolates with no insert in the *MFS1* promoter, 21 isolates displaying resistance to terbinafine (HR & MR)

were selected. Among the isolates carrying the type I insert, 24 isolates were randomly selected. In total, 138 strains were retained for precise resistance assessment.

The reference strains used in the assessment were as follows: for the sensitive reference, a selection of seven strains of our laboratory collection (Garnault et al, 2015 & 2019) isolated between 2012 and 2014 without insertion in P_{MFS1} and sensitive to terbinafine and tolnaftate at the discriminating concentration; for the P_{MFS1}-type I, type IIA and type III genotypes, strains with promotor replacements at the *MFS1 locus* in the sensitive reference strain IPO323 (P_{MFS1}-no insert) by either the P_{MFS1}- type I, type IIA or type III allele were used (Omrane et al, 2017).

For each of the 138 strains and the references, quantitative resistance to terbinafine was assessed as EC_{50} values (the concentration inducing 50% of the maximum fungicidal effect) through dose-response curves.

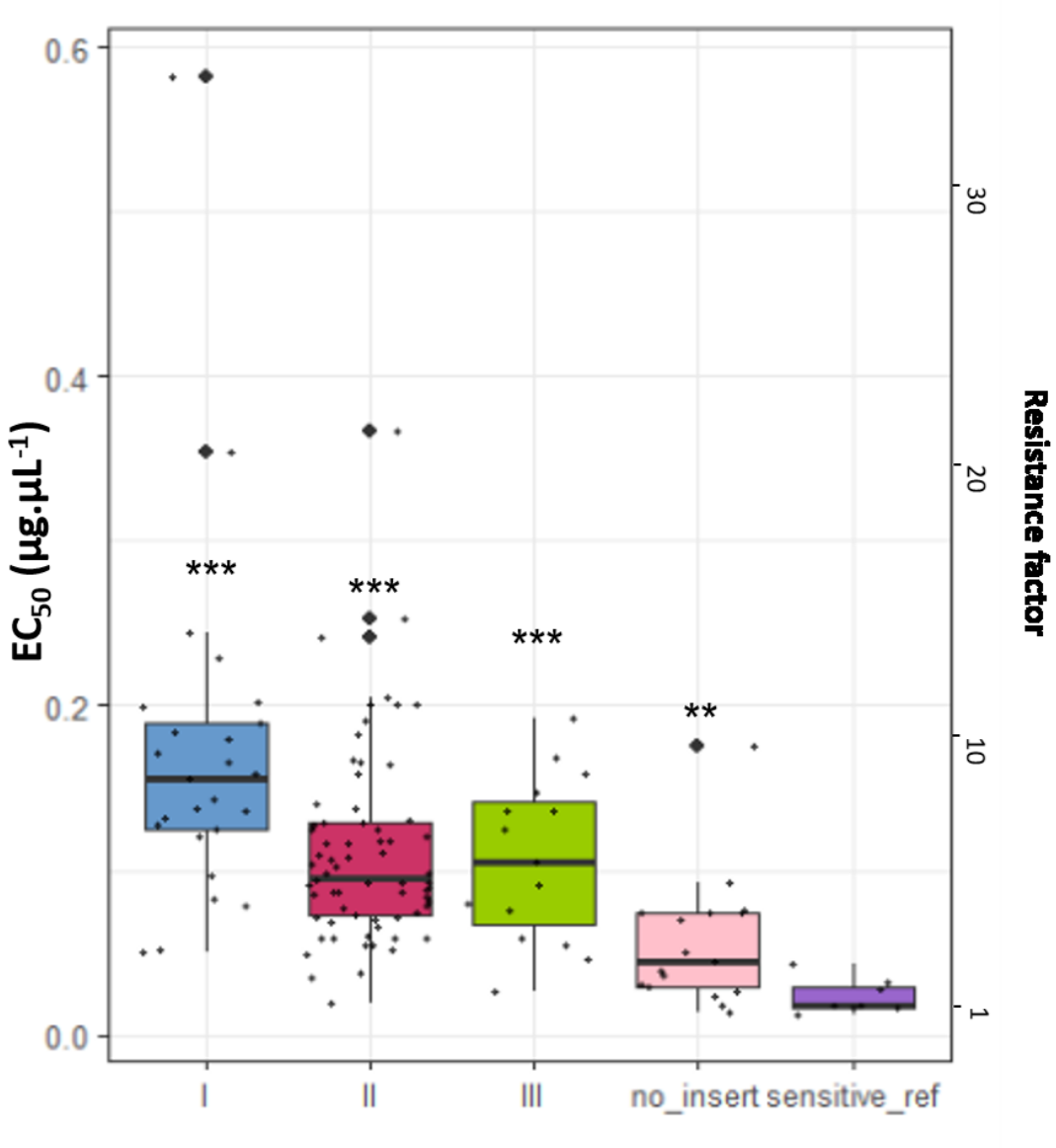

*Figure 3 Distribution of EC_{50} values to terbinafine for each genotype group: P_{MFS1}-type I, II and III, P_{MFS1}- no insert.-Sensitive references in these analyses are pooled values of seven sensitive strains. Each dot corresponds to the mean EC_{50} value of one strain. Student tests between sensitive reference and the other genotype were performed. Significant differences at p-value <0.005 are indicated by ** and p-value <0.0005 are indicated by ****

All P_{MFS1} genotype groups showed terbinafine resistance significantly different from the sensitive reference with mean resistance factors (RF) ranging from 3.1 to 9.4 (Fig. 3). Field isolates with the type I insert displayed the strongest resistance to terbinafine with a mean

RF of 9.4, followed by the field isolates with type II or type III inserts with an average RF of 7,7 and 5.84. It is noticeable that the EC_{50} values in each genotypic group were strongly dispersed.

Phenotypic diversity within a common genotype indicates additional resistance mutations

We then compared terbinafine resistance levels of isolates of the same P_{MFS1} genotype.

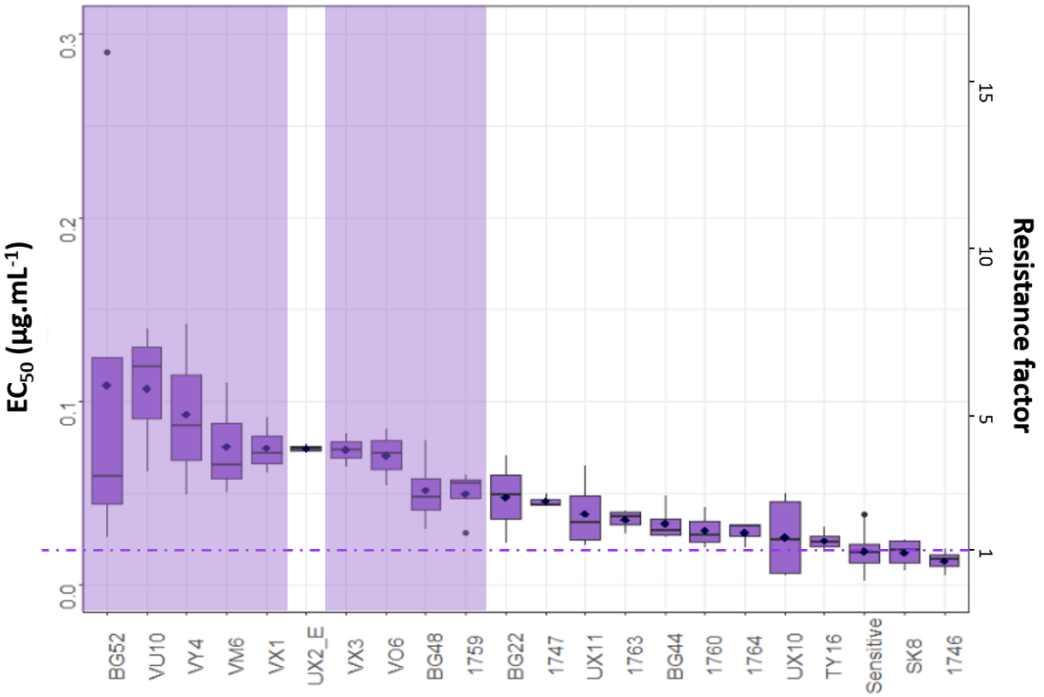

Figure 4: Distribution of terbinafine resistance profiles (EC_{50} & resistance factor) among isolates with P_{MFS1}-no_insert genotypes. The sensitive reference values used in the analysis were pooled from seven sensitive strains. The diamond-shaped dots represent the mean EC_{50} of each strain, while the horizontal lines represent the median EC_{50} value of the strain. ANOVA test with posthoc Bonferroni correction revealed significant differences from the sensitive reference as indicated by an the purple background for p-value <0.05. Resistance factors (RFs) were calculated based on the mean EC_{50} values

Among the strains without insert in $P_{MFS1,}$ we observed a quantitative distribution of the terbinafine EC_{50}-values (Fig. 4). According to the ANOVA test with Bonferroni correction, six strains (strains highlighted by the purple background) out of 14 were significantly different from the sensitive reference (with a resistance factor of 5 for strain VY4) indicating that terbinafine resistance can be obtained in an P_{MFS1}-no_insert background.

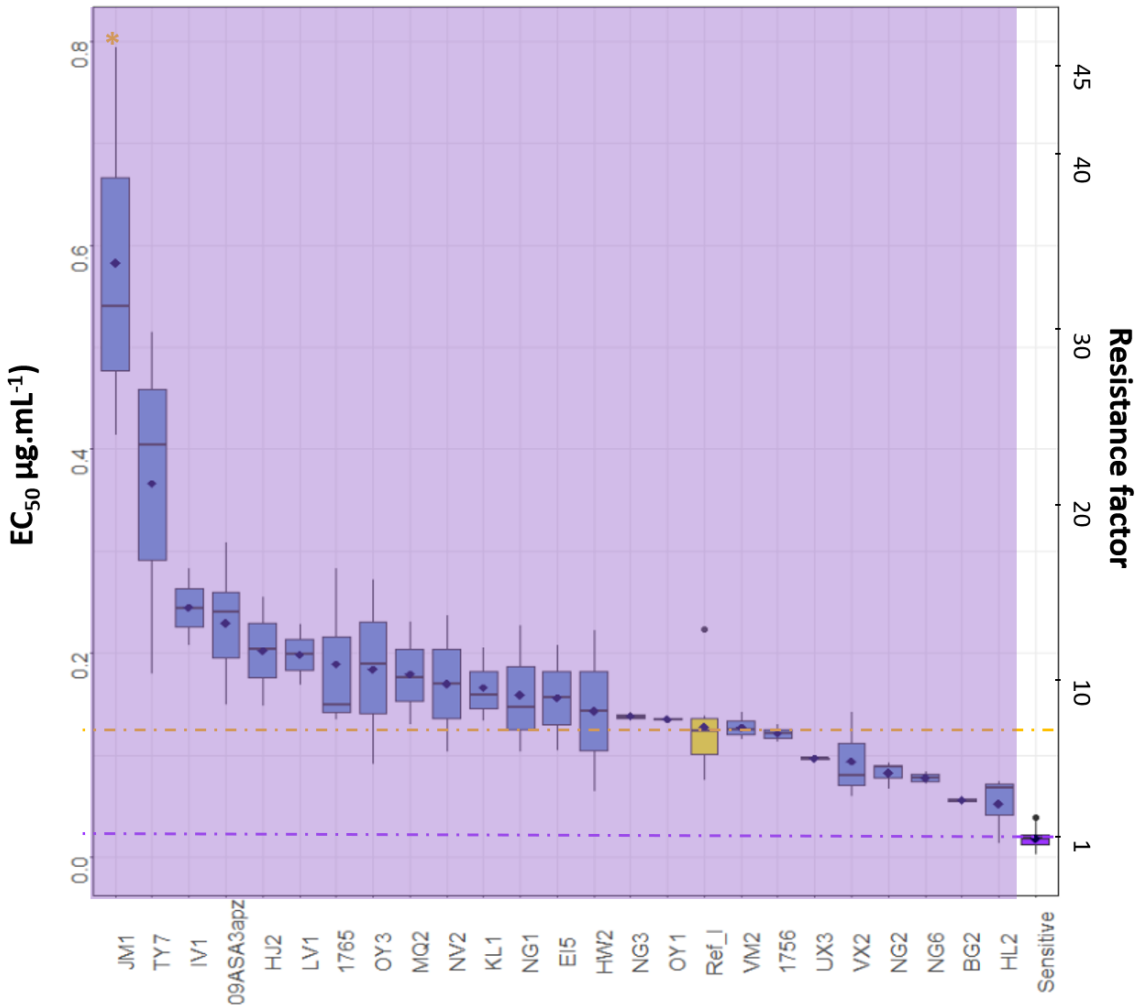

Figure 5 : Distribution of terbinafine resistance profiles (EC_{50} & resistance factor) among isolates with P_{MFS1}-type I genotypes. The sensitive reference values used in the analysis were pooled from seven sensitive strains. The yellow box indicate the EC_{50} values for the reference strain of the corresponding P_{MFS1}-type I genotype. The diamond-shaped dots represent the mean EC_{50} of each strain, while the horizontal lines represent the median EC_{50} value of the strain. ANOVA test with post-hoc Bonferroni correction revealed significant differences from the

sensitive reference as indicated by the purple highlighting background. for p-value <0.05. Significant differences from the P_{MFS1}-type I reference are indicated by a yellow asterisk (*), for p-value <0.05. Resistance factors (RFs) were calculated based on the mean EC_{50} values.

Among the 23 field strains with P_{MFS1}-type I genotype, all isolates showed significant differences in EC50 values compared to the sensitive reference (Fig. 5) including the P_{MFS1}-type I reference and the previously published strain 09-ASA-3apz (Omrane et al. 2015; Leroux et Walker, 2011). Resistance factors were heterogenic among strains. One isolate (JM1) displayed an EC_{50} value significantly different from the P_{MFS1}-type I reference strain. The resistance factor (RF) to terbinafine was 3-4 times higher in JM1 compared to the P_{MFS1}-type I reference strain and 34-fold higher than to the sensitive reference.

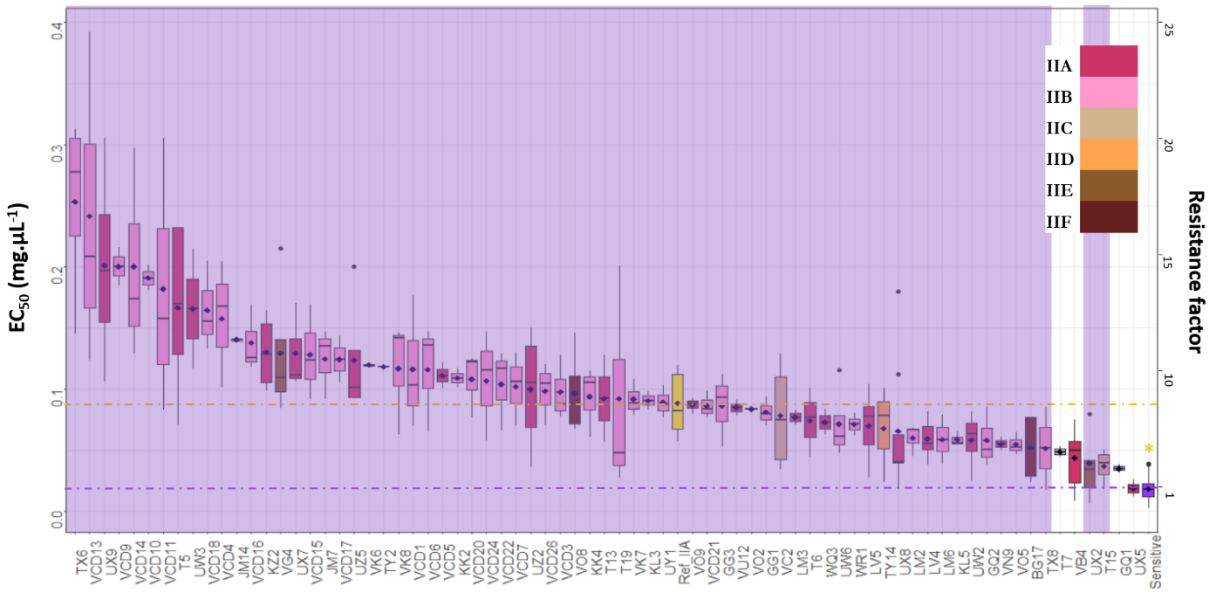

Figure 6 : Distribution of terbinafine resistance profiles (EC_{50} & resistance factor) among isolates with P_{MFS1}-type IIs genotypes. The sensitive reference values used in the analysis were pooled from seven sensitive strains. The yellow box indicates the EC_{50} values for the reference strain of the corresponding P_{MFS1}-type IIa genotype. The diamond-shaped dots represent the mean EC_{50} of each strain, while the horizontal lines represent the median

*EC_{50} value of the strain. ANOVA test with posthoc Bonferroni correction revealed significant differences from the sensitive reference as indicated by a highlighting frame, for p-value <0.05. Significant differences from the P_{MFS1}-*type *IIa reference were indicated by a yellow asterisk (*), for p-value <0.05. Resistance factors (RFs) were calculated based on the mean EC_{50} values.*

Among the 75 strains of P_{MFS1}-type II genotype 69 exhibited EC_{50} values significantly different from the sensitive reference (Figure 6, table S1). A quantitative distribution of EC_{50} values to terbinafine was observed among the strains. No significant difference of EC_{50}-values between the P_{MFS1}-type II reference and the tested isolates of the P_{MFS1}-type II genotype was observed, neither between the strains of P_{MFS1}-type IIA, B, C, D, E, or F genotype.

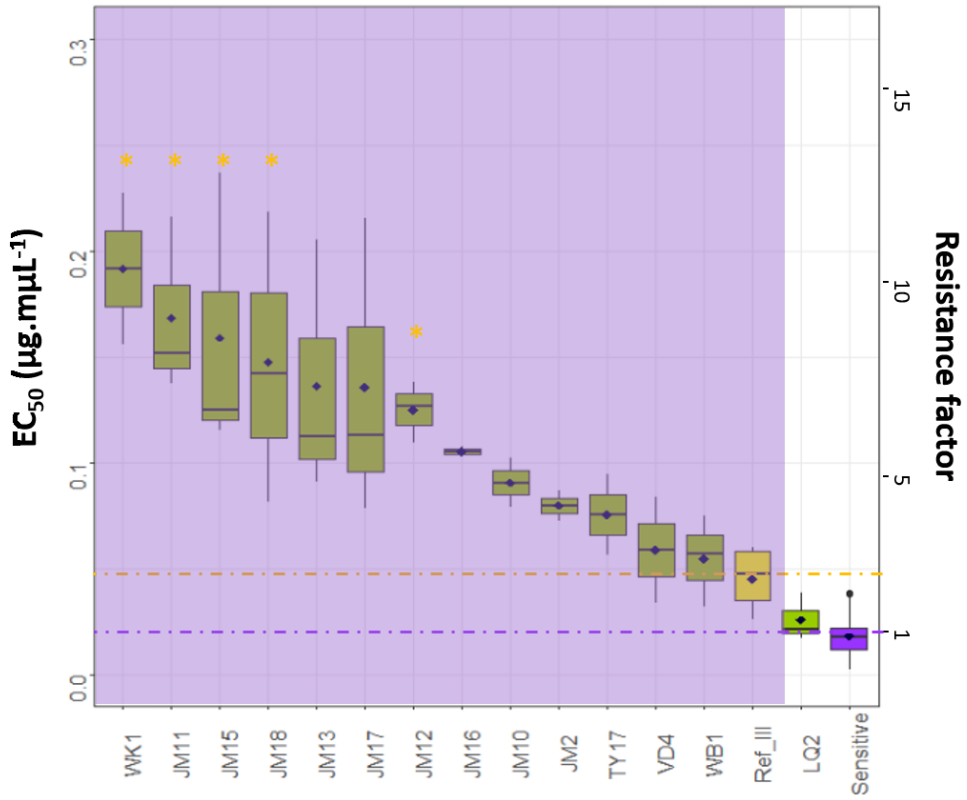

*Figure 7: Distribution of terbinafine resistance profiles (EC_{50} & resistance factor) among isolates with P_{MFS1}-*type *III genotypes. The sensitive reference values used in the analysis were pooled from seven sensitive strains. The*

yellow box indicates the EC_{50} values for the reference strain of the corresponding P_{MFS1}-type III genotype. The diamond-shaped dots represent the mean EC_{50} of each strain, while the horizontal lines represent the median EC_{50} value of the strain. ANOVA test with posthoc Bonferroni correction revealed significant differences from the sensitive reference as indicated by a highlighting frame, for p-value <0.05. Significant differences from the P_{MFS1}-type III reference were indicated by a yellow asterisk (*), for p-value <0.05. Resistance factors (RFs) were calculated based on the mean EC_{50} values.

The analyzed isolates of P_{MFS1}-type III genotype displayed quantitative distribution of terbinafine EC_{50} values (Fig. 7). According to the Anova test, 13 out of 14 isolates were significantly different from the sensitive reference with RFs between 2.5 and 10. Five strains significantly differed from the P_{MFS1}- type III reference strain, displaying 3-6 times higher EC_{50}-values.

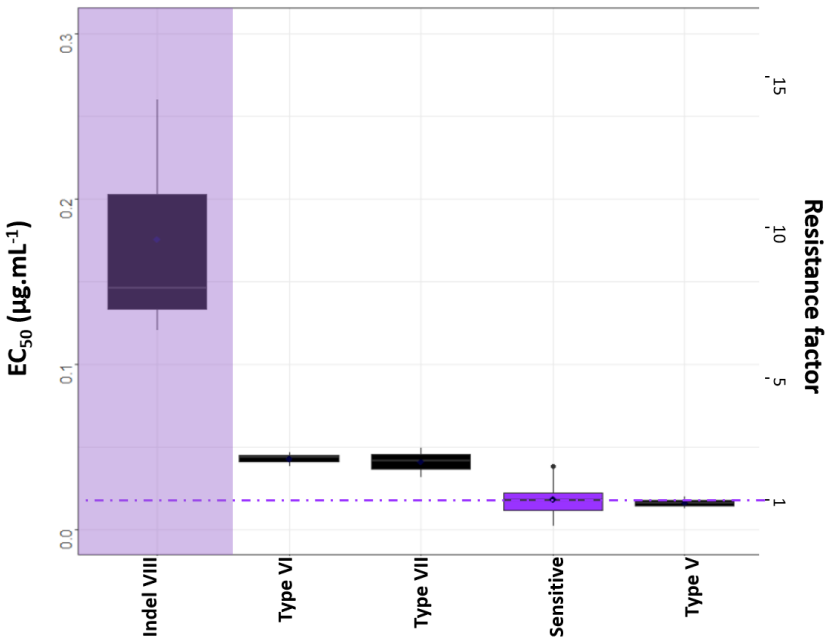

Figure 8: Distribution of terbinafine resistance profiles (EC_{50} & resistance factor) among isolates with P_{MFS1} type V, VI, VII and VIII genotypes. The sensitive reference values used in the analysis were pooled from seven sensitive

strains genotype. ANOVA test with posthoc Bonferroni correction revealed significant differences from the sensitive reference as indicated by a highlighting frame, for p-value <0.05.

Isolates with the type V, VI and VII inserts displayed EC_{50}-values ranging from 0.016 to 0.046 µg/mL statistically not different from the sensitive reference (Figure 8). These results indicate that these insertions in the promotor of *MFS1* do not confer resistance to terbinafine. On the opposite, isolate UW1 harbouring the indel VIII showed significant resistance to terbinafine (RF = 9.62 compared to the sensitive reference).

Taken together the results of the quantitative assessment of terbinafine resistance revealed the quantitative distribution of EC_{50} values for P_{MFS1} genotypes without insert, and with inserts of type I-II and III. For several strains (n=7 for P_{MFS1}-no insert, n=1 for P_{MFS1}-type I, n=5 for P_{MFS1}-type III) the RFs were significantly higher than of the corresponding reference strain indicating additional mutations involved in terbinafine resistance.

Among the new P_{MFS1} inserts, only type II inserts (C-E) and Indel VIII seem to confer terbinafine resistance.

Insert type VI does not confer terbinafine resistance

We chose to verify that insert type VI does not confer terbinafine resistance through the same gene-replacement strategy as published by Omrane et al, 2017. We introduced the corresponding replacement construct into the sensitive recipient strain IPO323. After PCR validation of hygromycin resistant transformants, three independent transformants carrying

the P_{MFS1}-type *VI* genotype were tested for their growth on terbinafine or tolnaftate. None out of the three transformants was able to grow at the discriminatory dose of the squalene-inhibitors (data not shown), confirming that insert number VI does not confer terbinafine resistance, neither MDR (see below).

Terbinafine resistance reflects multidrug resistance

As terbinafine or other squalene epoxidase inhibitors are not used in treatments against phytopathogenic fungi, we suspect that the observed resistances correspond to multi-drug resistance as previously observed by others (*Leroux et Walker, 2011; Kretschmer et al., 2009; Leroux et al., 2013)*.

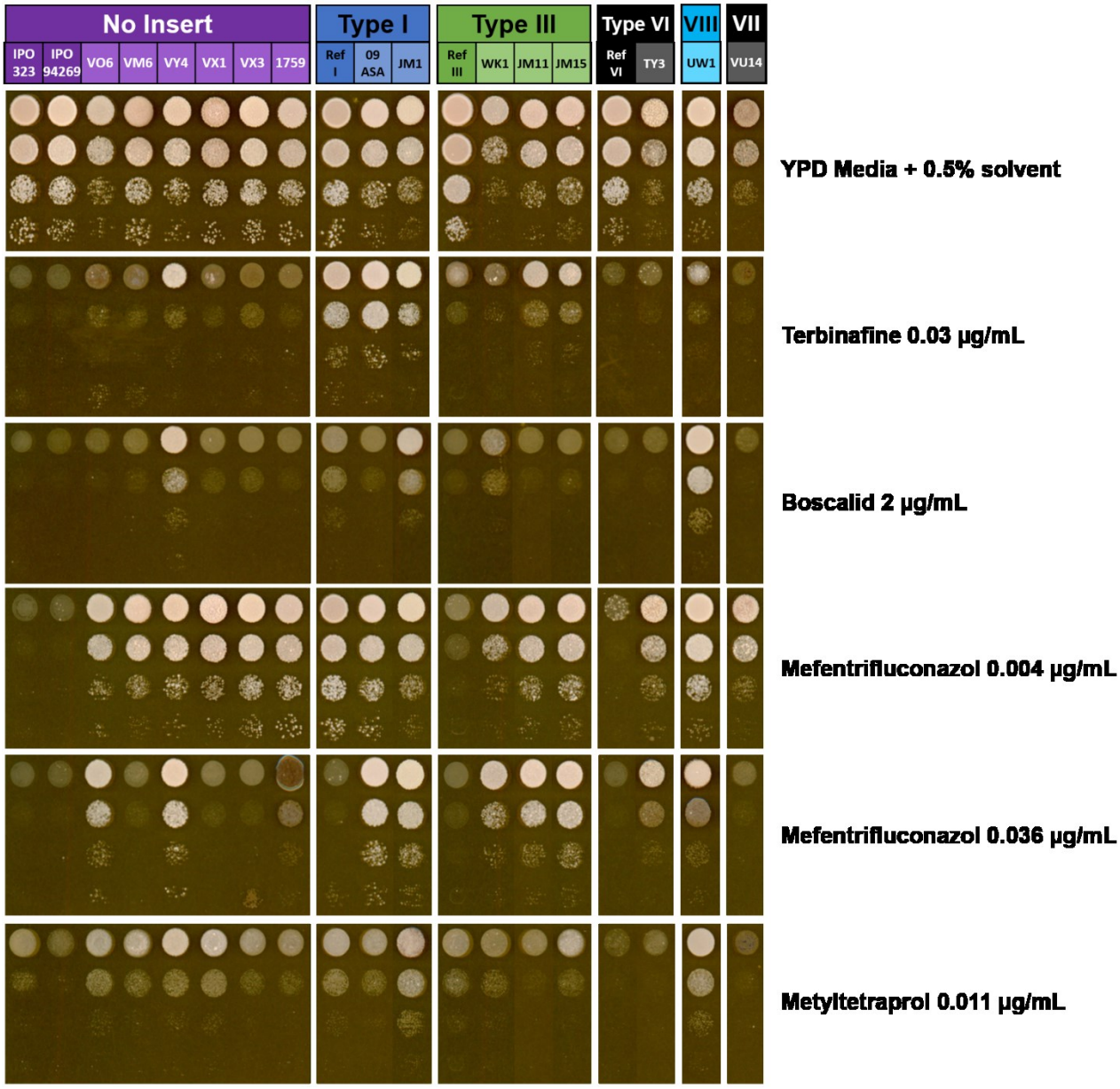

Figure 7 : Fungicide sensitivity assay of novel terbinafine resistant isolates. For a same genotype isolates from the field are represented with a lighter color than their corresponding reference.

To confirm that the accentuated terbinafine resistance of all strains that differ from their corresponding reference strain corresponds to an MDR phenotype (VO6, VM6, VY4, VX1, VX3, 1759 for the P_{MFS1}-*no insert* genotype, JM1 for the P_{MFS1}-type I genotype, WK1, JM11, JM15 for the P_{MFS1}-type III genotype; Figs. 4-7), we evaluated their sensitivity to fungicides of

different modes-of-action by a droplet growth assay. We also tested isolate UW1 (P_{MFS1}-Indel VIII) as well as strains with the insert types VI or VII, respectively, not conferring terbinafine resistance. As fungicides we tested the DMI mefentrifluconazole (Jørgensen et al., 2022; Kiiker et al., 2021; Vestergård et al., 2023) , the SDHI boscalid , as well as a complex III inhibitor, QoI-A, metyltetraprole. This last fungicide is not yet concerned by specific resistance to QoI due to known target site modification in *Z. tritici* field populations (Matsuzaki et al., 2020).

Fig. 9 shows the growth of all tested strains on control and test media. On high terbinafine concentration (0.03 µg/mL), only strains with RF > 5 were able to grow: VY4 the only strain of genotype P_{MFS1}-*no_insert*, all strains of P_{MFS1}-type *I*, P_{MFS1}-type *III* genotype strains JM11 &JM 15, P_{MFS1}-*Indel VIII* strain UW1. As expected, the strains of genotype P_{MFS1}-type *VI & VII* did not grow.

On boscalid at 2 µg.mL^{-1}, disparities in growth emerged between VY4 and the P_{MFS1}-no insert references IPO323 and IPO94269, as well as between JM1 and the P_{MFS1}-type I reference. Also strain UW1 (P_{MFS1}-*Indel VIII*) was resistant to this SDHI. At low concentration of mefentrifluconazole (0.004 µg/mL), one can notice that only the elder sensitive reference strains did not grow, *i.e.* IPO323, IPO94269 as well as the IPO323 based P_{MFS1}-type *III* reference strain. However, IPO323 based reference P_{MFS1}-type *I* strain showed resistance to this DMI at low concentration showing that this MDR genotype confers resistance to mefentrifluconazole. The growth of the non-MDR strains TY3 and VU14 (type VI & VII inserts), on the opposite, hint to specific resistance, probably through *CYP51* modification. At higher concentration (0.036 µg.mL^{-1}of mefentrifluconazole), differences between strains of a

common P_{MFS1} genotype appeared, namely between VO6, VY4 and the P_{MFS1}-no insert references; 09ASA-3apz and JM1 relative to the P_{MFS1}-type I reference; between P_{MFS1}-type III field strains and their corresponding reference. These differences support the hypothesis that MDR and target site modification increase the resistance level to this DMI.

Growth differences were less striking on metyltetraprole containing medium. The sensitive controls IPO323, IPO94269, and the type VI & VII strains TY3 and VU14 were sensitive to metyltetraprole (Fig. 7). Resistance, visible as growth was observed for strain UW1 (Indel VIII). Concerning strains of common genotype: those without insert in $P_{MFS1,}$ namely VO6, VM6, VY4, and VX1 demonstrated increased growth compared to the sensitive references IPO94269 and IPO323; as does JM1 relative to the P_{MFS1}-type I reference.

In conclusion, strains with enhanced terbinafine resistance displayed increased resistance to fungicides with unrelated modes of action, thereby indicating that terbinafine resistance reflects multidrug-resistant (MDR) phenotype. This holds true especially for strains VO6 & VY4 (no-insert), JM1 (type I), and UW1 (Indel VIII). The droplet growth-test in Fig. 7 also shows that the type VI insert does not confer MDR, visible through the absence of growth of IPO323 transformant Trf-VI on all tested fungicides.

Discussion

In this study we observed a large diversity of P_{MFS1} alleles within our *Z. tritici* population 2020-2021 sampled as terbinafine resistant isolates. Notably, apart from the type VIII indel and type V, all described inserts, both in previous studies and in our research, exhibited characteristics of transposable elements (TE). In addition, we noted that different individuals sharing the same P_{MFS1} allele, displayed distinct terbinafine resistance levels.

Strains exhibiting notable resistance to terbinafine also display resistance to the fungicide metyltetraprol unaffected by known mutations conferring resistance to QoIs, but is significantly affected by MDR (Matsuzaki et al., 2020), as well as to the DMI mefentrifluconazol and/or the SDHI boscalid. This is the case for the type I reference strain, associating terbinafine resistance with resistance to metyltetraprol. Strain UW1 with the novel genotype P_{MFS} -Indel VIII, resistant to terbinafine, also exhibited resistance to metyltetraprol. The use of the clinical squalene epoxidase inhibitor fungicide, terbinafine, has been shown to be an effective approach for assessing multidrug resistance (MDR) in the field. At this stage, this can be confirmed through metyltetraprol resistance assays.

Large diversity of P_{MFS1} alleles

In total, our study has identified six new inserts (type IID to F, type VI to VIII) within the *MFS1* promoter region. This increases the total count of inserts found in this region to 13 when considering previous research (Omrane et al., 2017; Mäe et al., 2020; Lavrukaitė et al., 2023). The high frequency of inserts in P_{MFS1} suggests that the zone of 360 bp, located

between -108 and – 468 relative to the start codon, is a hotspot for insertions. In particular, our analysis showed the presence of at least seven different inserts at locus -468, with four of them showing high similarity to the previously identified type II inserts (A & B, Omrane et al., 2017). The similarity among the six type II inserts suggests a common ancestral insertion event that underwent several mutations or rearrangements leading to the observed insert genotypes.

Despite the diversity of inserts found in P_{MFS1}, our results show that among all described inserts only indel VIII and inserts I, II (5 in total), and III confer an MDR phenotype. These last three types account for 92% of the MDR strains identified in France between 2020 and 2021 (Type I, 72%; Type II, 14%; Type III, 6%). In contrast, the remaining inserts (Types IV to VII, found only in one isolate for each allele) do not provide resistance.

Insert origins

Our analysis of *Z. tritici* isolates from 2020-2021 has revealed two novel inserts displaying similarities with miniature inverted-repeat transposable elements (MITEs): type VI and type VII. The latter was discovered in an isolate from France in 2021, at the same locus (-468) as the previously reported Type II inserts, which also share conserved domains with retrotransposons classified as RLSX_LARD_gridr. In a previous study, the type I insert was described as an LTR retrotransposon, type IV as a transposon, and upon further analysis, we found that type II and III inserts display similarities with retrotransposons and transposons respectively. Except for insert types V and VIII, all the inserts found and described appear to originate from transposition events. These transposition events may have occurred at

different times; the type II insert may be the oldest, as evidenced by the accumulation of mutations (type IIA to F). While the type I insert seems to be one of the most recent insertions, given its 100% sequence conservation among isolates with the P_{MFS1}-type I insert genotype in our sampling. These inserts, detected in France in 2020 and 2021, underline once again the promoter region's plasticity in field strains and suggest that more new insert discoveries are yet to be made in this field.

Previous studies have shown that putative pathogenicity-encoding genes can be found associated with TE-rich regions in *Z. tritici* (Dhillon et al., 2014). In *Leptosphaeria maculans 'brassicae,'* TEs play a role in pathogen adaptation, impacting effector gene regulation (Grandaubert et al., 2014). Under stress, TEs impact gene expression dynamics in pathogens like *Z. tritici* (Fouché et al., 2020). During the plant infection process, pathogens rely on the epigenetic control of virulence factors by derepressing nearby TEs, leading to genome size expansions (Fouché et al., 2022). Hence, the presence of TEs in PMFS1 could originate from a TE burst associated with the stress involved in the plant infection process and could have been selected due to environmental pressure from fungicides in the field.

In summary we have identified and characterized four distinct insert types with potential transposition origins (IV, V, VI, and VII) as non-multidrug resistant (no-MDR). Notably, these non-MDR inserts have been found only once. In contrast, we observed that isolates from the field containing inserts associated with potential transposition events linked to multidrug resistance (types I, II, III) were the most frequent within our sample. This finding suggests

that, despite the presence of a transposition hotspot in P_{MFS1}, the resulting inserts do not consistently lead to an MDR phenotype. It is likely that isolates with inserts conferring MDR are preferentially selected in the field during fungicide treatments, as the MDR phenotype provides a fitness advantage by enhancing fungicide tolerance. Hence, the high number of isolate found in the field displaying P_{MFS1} *geno*type linked to the MDR phenotype.

Another new P_{MFS1} allele, which we have named P_{MFS} -Indel VIII, has been discovered. This allele exhibits a 678 bp deletion, removing 58 bp out of 166 bp from the 5'UTR region. Additionally, a 164 bp insert is linked to this deletion, which is conserved in the *Z. tritici* genome but does not share any similarity with known transposable element structures. The unique Isolate with P_{MFS} -Indel VIII displayed significant resistance to terbinafine. These findings suggest an MDR mechanism at play, linked to an insertion-deletion within the 5'UTR region.

Our findings underscore that evaluating the MDR potential in the field cannot be based solely on the genotyping of the P_{MFS1} promoter size; specific primers must be used to target the sequences of the inserts that confer resistance. Otherwise, MDR potential must be evaluated through phenotyping.

Phenotype - genotype discrepancy suggests additional mechanisms involved in MDR

Several isolates from our collection displayed higher resistance factors (RFs) than their respective reference strains for the same genotypes, including five for P_{MFS1}-Type III, one for

P_{MFS1}-Type I and six for P_{MFS1}-no insert. This discrepancy suggests the existence of potential additional mechanisms of multidrug resistance (MDR) that may operate independently of the *MFS1* promoter insert. These mechanisms may involve mutations outside the promoter region of *MFS1*, such as gain-of-function mutations in transcription factors, as previously reported in *Clarireedia homoeocarpa* (Sang et al., 2018) and *Botrytis cinerea* (Kretschmer et al., 2009), or unidentified quantitative mutations of resistance.

Noticeably, our study found that the previously described P_{MFS1}-Type I wild-type strain (MDR6/09ASA), which exhibited the highest resistance factor towards terbinafine in the study by Omrane et al. (2017), displayed an RF of 15, while an isolate with the same genotype exhibited an RF of 30. Overall, the MDR phenotype observed in our field isolates displayed higher levels of resistance than those reported in previous studies . These findings suggest that the mechanisms underlying MDR in *Z. tritici* field isolates may be more complex and diverse than previously thought, and may involve multiple genetic factors. Further investigation is needed to elucidate these mechanisms and to develop more effective strategies for managing multidrug resistance in *Z. tritici* field strains.

Material and Method

***Z. tritici* strain collection**

French field strains used in this study were obtained from the "Performance Network" (Garnault et al., 2019) during the years 2020 and 2021. Both French and British strains in our panel were isolated from infected wheat leaves and suspended in water. The spore suspensions were incubated at 18°C in the dark for 24 hours on PDA media supplemented with the discriminatory concentration of terbinafine (0.015 µg/mL) (Leroux & Walker, 2011).

After incubation, colonies with long germ tubes were picked using a sterile toothpick and isolated three to five times on PDA media supplemented with antibiotics (Kanamycin, Streptomycin, and Penicillin (Sigma-Aldrich) at 37.5 µg/mL). Pure strains were stored as spore suspensions in 25% glycerol at -80°C. Strains from Belgium, Denmark, Estonia, Germany, Ireland, and Lithuania were provided by different colleagues as pure strains based on their respective P_{MFS1} genotypes.

Reference strains

In this study, one of the sensitive *Z. tritici* reference strains used was IPO323, which is susceptible to all fungicides and recognized as a worldwide reference (Goodwin et al., 2011). To establish the basal EC_{50} value to terbinafine, as sensitive reference we selected six field strains of our collection, isolated between 2012 and 2014 of P_{MFS1}-no-insert genotype, sensitive to terbinafine (not germinating on PDA at the terbinafine discriminatory dose), in addition to IPO323. Transformants carrying either the P_{MFS1}-type I allele, P_{MFS1}-type II allele, or P_{MFS1}-Type III allele integrated at the *MFS1 locus* of IPO323 (Omrane et al., 2017) were employed as references and named Ref-I, Ref-II, and Ref-III, respectively. The full list of reference strains and field isolates used in this study is provided in Table S1.

General growth conditions

For the precultures, strains were taken out of the -80°C and plated on solid YPD medium (20 $g.L^{-1}$ dextrose, 20 $g.L^{-1}$ peptone, 10 $g.L^{-1}$ yeast extract, 10 $g.L^{-1}$ agar). All strains were grown in 10 mL liquid YPD medium in 50 mL sterilized Erlenmeyer flasks plugged with cotton wool for 7 days at 150 rpm and 18°C in the dark. Cell concentrations were determined by OD

measurements at λ=405 nm in a Spectramax M2 microtiterplate reader (Molecular Devices, USA) according to the formula established by Ballu *et al*. (2021).

Qualitative resistance assay to fungicides (droplet growth test)

The qualitative assessment of terbinafine resistance as proxy for the MDR phenotype for the 398 isolates was performed using a droplet test according to the following conditions. To this end, suspensions of 10^7, 10^6, 10^5, and 10^4 spores.mL-1 respectively were deposited as drops in columns on 12 cm square Petri dishes containing solid YPD medium supplemented with antibiotics (Kanamycin, Streptomycin, and Penicillin (Sigma-Aldrich) at 37.5 µg.mL^{-1}) and a range of terbinafine concentrations (0.015, 0.03, and 0.06 µg.mL^{-1}) or solvent (DMSO at 0.5% v/v). All fungicides were supplied as 200 X concentrated DMSO or ethanol solutions. Fungal growth was observed after 7 days. For each strain and each terbinafine concentration, a score was given ranging from 0 (no growth) to 4 (growth at the lowest spore concentration) . The resistance profile was determined by concatenating the independent scores obtained for the tested modalities, starting at the lowest terbinafine concentration, ranging from 000 to 444. Strains with a resistance profile between 300 and 400 were categorized as highly resistant (HR), strains with a resistance profile between 200 and 300 were categorized as mid-resistant (MR), strains with a resistance profile between 100 and 200 were categorized as low-resistant (LR), and strains with a resistance profile below 100 were categorized as sensitive (S), prior to EC_{50} establishment (following section). Quantitative resistance assay to fungicide were also conducted with fungicide mefentrifluconazole (0.004 µg/mL ; 0.036 µg/mL) boscalid (2 µg/mL) and metyltetraprole (0.011 µg/mL).

Quantitative terbinafine resistance assessment (EC_{50} determination through dose response curve)

After quantifying spore concentrations, pre-cultures of 138 field isolates and reference strains were adjusted to 1.25 × 10^6 spores/mL in 200 µL of YPD medium supplemented with antibiotics (Kanamycin, Streptomycin (Sigma-Aldrich) 37,5 µg/mL) supplemented with 0.5% v/v DMSO (Control) or terbinafine diluted in DMSO (0.5% of the final volume). Different terbinafine concentrations were used for high resistance (HR) and low resistance (LR) strains (table S1). A breathable film (Breathe-easy®; Diversified Biotech) was applied, and the isolates were incubated at 18°C and 150 rpm in a microplate shaker (Innova S44i, Eppendorf). Three biological replicates, each with three technical replicates, were performed for each isolate. After 7 days of growth, cell concentrations were determined by measuring the absorbance at 405 nm. Data were analyzed using R software (R core team, 2018; version 4.1.3) and a customized script (Ballu, unpublished), utilizing the drc package. Growth at each terbinafine concentration relative to the control medium was calculated using the formula:

(Cell concentration at dose x) / (Cell concentration in control medium)

The drm function was employed to model dose-response curves using a four-parameter Log-Logistic function, allowing determination of the EC50 for terbinafine (the concentration inducing 50% of the maximum fungicidal effect) for all isolates and biological replicates. Comparisons between replicates were made using the EDcomp function to identify any significant differences. Average EC50 values were analyzed via ANOVA (car package) on

log-transformed data, and a Bonferroni post-hoc test was performed after confirming the normality and homoscedasticity of model residuals.

P_{MFS1} genotyping

After 7 days of growth on YPD agar media, 50 – 100 mg of fresh culture was harvested per strain, placed in a microtiter plate and immediately frozen at -80°C. Cell lysis was performed mechanically twice in AP1 buffer + Rnase A and reagent DX (Qiagen) using tungsten beads in MIXER MILL MM 400 homogenizer (RETSCH®) at 20 Hz for 20 seconds. DNA was precipitated with sodium acetate pH 5 at 0.5 M final concentration and the addition of 0.7 vol of isopropanol. After centrifugation, dry DNA was resuspended in AE buffer (Qiagen). Genotyping of the *MFS1* promotor was performed on all 398 strains by PCR using the primer pair P_{MFS1}_2F and P_{MFS1}_4R (Omrane et al 2017). All isolates with the P_{MFS1}-Type II, P_{MFS1}-Type III alleles, 16 isolates with P_{MFS1}-no insert allele and 21 isolates with P_{MFS1}-type I insert allele were sequenced with the Sanger protocol (by Eurofins Genomics, Köln, Germany).

Sequence analysis

Sequenced promoters of *MFS1* of field isolated were aligned using with the P_{MFS1} sequences of the reference strains IPO323, and the sequences of reference P_{MFS1}-types I, II, and III. Any inserts found that did not align with the known inserts in P_{MFS1} were aligned to the annotated reference genome of *Zymoseptoria tritici*, with transposable element annotation from (Badet et al., 2020; Oggenfuss et al., 2021), and were qualified as potential TEs if the 80-80-80 rule was met (Wicker et al., 2007).

***MFS1* gene replacement constructs**

To introduce the MFS1 type V - MDR allele into the sensitive IPO323 strain, a replacement cassette was constructed using the same strategy described in Omrane et al. (Omrane et al. 2017) with minor change. 5' promotor and 3' terminator sequence of MFS1 in TY3 *Z.tritici* strain were obtain by 2 PCR with primer seq_prom_for/ seq_prom_rev and seq_term_for/ seq_term_rev and sanger sequencing (Eurofins, Luxembourg) with same primers. For all PCR performed to obtain cloning fragments, the Taq polymerase Phusion® (Thermo Fisher Scientific Inc., Waltham, MA, USA) was used under adapted PCR conditions using primers referenced in Table S.2. The MFS1 allele, 1,273 bp upstream until 510 bp downstream of the open reading frame (ORF), was amplified from TY3 strain DNA (4C6) with the primer pair MDR6-7_pKr_F/ Gibs_MDRIV_R. A 737-bp 3' flank of the MFS1 gene to facilitate homologous recombination was amplified from IPO323 genomic DNA with primers Ipo323_hyg_F and Ipo323_pKr_R. Finally, the hygromycin resistance marker gene hph was amplified from plasmid pCAMB-HPT-Hind (Kramer et al., 2009) with the primer pair Gibs_Hygro_for/Hygro_ipo323_R. The three fragments (0.05 pmol each) were assembled with XhoI-EcoRI-digested pCAMB-HPT-Hind (0.05 pmol) using the Gibson Assembly Cloning kit (New England Biolabs, Ipswich, MA, USA) according to the supplier's instructions. NEB 5-alpha competent *E. coli* (High Efficiency) (New England Biolabs, Ipswich, MA, USA) were transformed by heat shock with 2µl of the assembly reaction mixture. Successfully transformed colonies were selected on medium added with kanamycin (50mg.L^{-1}) then validated by PCR on colonies with 3 pairs of primers pCAMBIA_rev/MFS1_rev, MFS1_for/pHygro_rev and pHygro_for/pCAMBIA_for. Positive clones were picked for plasmid extractions and mini-

prepped plasmid construct was validated by Sanger sequencing (Eurofins, Luxembourg) with primers listed on table S.2.

Agrobacterium tumefaciens strain AGL1 was transformed by heat shock with the generated plasmid pCAMBIA0380_RH_pMFS1_V_MFS1_hygro. Positive colonies were selected on YEB broth (beef extract 5g.L^{-1}, yeast extract 1g.L^{-1}, peptone 5g.L^{-1}, saccharose 5g.L^{-1}, MgCl2 0,5g.L^{-1}) with rifampicin (50mg.L^{-1}), kanamycin (50mg.L^{-1}), and ampicillin (100mg.L^{-1}) then screened by same colonies PCR as on *E.coli*.

ACKNOWLEDGEMENTS:

This work was supported by Anova-Plus Company. The authors would like to thank the Performance Network for supplying leaf samples in 2020-2021

References:

Badet, T., Oggenfuss, U., Abraham, L., McDonald, B. A., & Croll, D. (2020). A 19-isolate reference-quality global pangenome for the fungal wheat pathogen Zymoseptoria tritici. *BMC Biology*, *18*(1), 1–18. https://doi.org/10.1186/s12915-020-0744-3

Ballu, A., Deredec, A., Walker, A. S., & Carpentier, F. (2021). Are efficient-dose mixtures a solution to reduce fungicide load and delay evolution of resistance? An experimental evolutionary approach. *Microorganisms*, *9*(11). https://doi.org/10.3390/microorganisms9112324

Dhillon, B., Gill, N., Hamelin, R. C., & Goodwin, S. B. (2014). The landscape of transposable elements in the finished genome of the fungal wheat pathogen Mycosphaerella graminicola. *BMC Genomics*, *15*(1), 1–17. https://doi.org/10.1186/1471-2164-15-1132

Fones, H., & Gurr, S. (2015). The impact of Septoria tritici Blotch disease on wheat: An EU perspective. *Fungal Genetics and Biology*, *79*, 3–7. https://doi.org/10.1016/J.FGB.2015.04.004

Fouché, G., Rosati, D., Venet, C., Josserand, H., Latorse, M. P., Debieu, D., & Fillinger, S. (2022). LC-MS/MS-Based Fungicide Accumulation Assay to Demonstrate Efflux Activity in the Wheat Pathogen Zymoseptoria tritici. *Microorganisms*, *10*(8). https://doi.org/10.3390/microorganisms10081494

Fouché, S., Badet, T., Oggenfuss, U., Plissonneau, C., Francisco, C. S., & Croll, D. (2020). Stress-Driven Transposable Element De-repression Dynamics and Virulence Evolution in a Fungal Pathogen. *Molecular Biology and Evolution*, *37*(1), 221–239. https://doi.org/10.1093/molbev/msz216

Fouché, S., Oggenfuss, U., Chanclud, E., & Croll, D. (2022). A devil's bargain with transposable elements in plant pathogens. *Trends in Genetics*, *38*(3), 222–230. https://doi.org/10.1016/j.tig.2021.08.00

Garnault, M., Duplaix, C., Leroux, P., Couleaud, G., Carpentier, F., David, O., & Walker, A. (2019). Spatiotemporal dynamics of fungicide resistance in the wheat pathogen *Zymoseptoria tritici* in France. *Pest Management Science*, *July 2018*, ps.5360. https://doi.org/10.1002/ps.5360

Grandaubert, J., Lowe, R. G. T., Soyer, J. L., Schoch, C. L., Van De Wouw, A. P., Fudal, I., Robbertse, B., Lapalu, N., Links, M. G., Ollivier, B., Linglin, J., Barbe, V., Mangenot, S., Cruaud, C., Borhan, H., Howlett, B. J., Balesdent, M. H., & Rouxel, T. (2014). Transposable element-assisted evolution and adaptation to host plant within the Leptosphaeria maculans-Leptosphaeria biglobosa species complex of fungal pathogens. *BMC Genomics*, *15*(1), 1–27. https://doi.org/10.1186/1471-2164-15-891

Hu, M., & Chen, S. (2021). Non-target site mechanisms of fungicide resistance in crop pathogens: A review. *Microorganisms*, *9*(3), 1–19. https://doi.org/10.3390/microorganisms9030502

Huf, A., Rehfus, A., Lorenz, K. H., Bryson, R., Voegele, R. T., & Stammler, G. (2018). Proposal for a new nomenclature for CYP51 haplotypes in Zymoseptoria tritici and analysis of their distribution in Europe. *Plant Pathology*, *67*(8), 1706–1712. https://doi.org/10.1111/ppa.12891

Jørgensen, L. N., Matzen, N., Heick, T. M., O'Driscoll, A., Clark, B., Waite, K., Blake, J., Glazek, M., Maumene, C., Couleaud, G., Rodemann, B., Weigand, S., Bataille, C., R, B., Hellin, P., Kildea, S., & Stammler, G. (2022). Shifting sensitivity of septoria tritici blotch compromises field performance and yield of main fungicides in Europe. *Frontiers in Plant Science*, *13*(November), 1–17. https://doi.org/10.3389/fpls.2022.1060428

Kiiker, R., Juurik, M., Heick, T. M., & Mäe, A. (2021). Changes in dmi, sdhi, and qoi fungicide sensitivity in the estonian zymoseptoria tritici population between 2019 and 2020. *Microorganisms*, *9*(4), 1–15. https://doi.org/10.3390/microorganisms9040814

Klink, H., Verreet, J. A., Hasler, M., & Birr, T. (2021). Will Triazoles Still Be of Importance in Disease Control of Zymoseptoria tritici in the Future? *Agronomy 2021, Vol. 11, Page 933*, *11*(5), 933. https://doi.org/10.3390/AGRONOMY11050933

Kretschmer, M., Leroch, M., Mosbach, A., Walker, A. S., Fillinger, S., Mernke, D., Schoonbeek, H. J., Pradier, J. M., Leroux, P., De Waard, M. A., & Hahn, M. (2009). Fungicide-driven evolution and molecular basis of multidrug resistance in field populations of the grey mould fungus Botrytis cinerea. *PLoS Pathogens*, *5*(12). https://doi.org/10.1371/journal.ppat.1000696

Lapalu, N., Lamothe, L., Petit, Y., Genissel, A., Delude, C., Feurtey, A., Abraham, L. N., Smith, D., King, R., Renwick, A., Sucher, J., Steindorff, A. S., Goodwin, S. B., Grigoriev, I. V, Hane, J., Rudd, J., Croll, D., Scalliet, G., Lebrun, M., … Genomics, E. (2023). *Zymoseptoria tritici*.

Lavrukaitė, K., Heick, T. M., Ramanauskienė, J., Armonienė, R., & Ronis, A. (2023). Fungicide sensitivity levels in the Lithuanian Zymoseptoria tritici population in 2021. *Frontiers in Plant Science*, *13*(January), 1–10. https://doi.org/10.3389/fpls.2022.1075038

Leroux, P., Gredt, M., Remuson, F., Micoud, A., & Walker, A. S. (2013). Fungicide resistance status in French populations of the wheat eyespot fungi Oculimacula acuformis and Oculimacula yallundae. *Pest Management Science*, *69*(1), 15–26. https://doi.org/10.1002/ps.3408

Leroux, P., & Walker, A. S. (2011). Multiple mechanisms account for resistance to sterol 14α-demethylation inhibitors in field isolates of Mycosphaerella graminicola. *Pest Management Science*, *67*(1), 44–59. https://doi.org/10.1002/ps.2028

Lucas, J. A., Hawkins, N. J., & Fraaije, B. A. (2015). The Evolution of Fungicide Resistance. In *Advances in Applied Microbiology* (Vol. 90). Elsevier. https://doi.org/10.1016/bs.aambs.2014.09.001

Mäe, A., Fillinger, S., Sooväli, P., & Heick, T. M. (2020). Fungicide Sensitivity Shifting of Zymoseptoria tritici in the Finnish-Baltic Region and a Novel Insertion in the MFS1 Promoter. *Frontiers in Plant Science*, *11*, 0–10. https://doi.org/10.3389/fpls.2020.00385

Matsuzaki, Y., Kiguchi, S., Suemoto, H., & Iwahashi, F. (2020). Antifungal activity of metyltetraprole against the existing QoI-resistant isolates of various plant pathogenic fungi: Metyltetraprole against QoI-R isolates. *Pest Management Science*, *76*(5), 1743–1750. https://doi.org/10.1002/ps.5697

Möller, M., & Stukenbrock, E. H. (2017). Evolution and genome architecture in fungal plant pathogens. *Nature Reviews Microbiology 2017 15:12*, *15*(12), 756–771. https://doi.org/10.1038/nrmicro.2017.76

Oggenfuss, U., & Id, D. C. (2023). *Recent transposable element bursts are associated with the proximity to genes in a fungal plant pathogen*. 1–25. https://doi.org/10.1371/journal.ppat.1011130

Omrane, S., Audéon, C., Ignace, A., Duplaix, C., Aouini, L., Kema, G., Walker, A.-S., & Fillinger, S. (2017). Plasticity of the MFS1 Promoter Leads to Multidrug Resistance in the Wheat Pathogen Zymoseptoria tritici . *MSphere*, *2*(5), 1–18. https://doi.org/10.1128/msphere.00393-17

Omrane, S., Sghyer, H., Audéon, C., Lanen, C., Duplaix, C., Walker, A. S., & Fillinger, S. (2015). Fungicide efflux and the MgMFS1 transporter contribute to the multidrug resistance phenotype in Zymoseptoria tritici field isolates. *Environmental Microbiology*, *17*(8), 2805–2823. https://doi.org/10.1111/1462-2920.12781

Sang, H., & Hulvey, J. P. (2018). *A Xenobiotic Detoxification Pathway through Transcriptional Regulation in Filamentous Fungi*. *9*(4), 1–17.

Singh, N. K., Badet, T., Abraham, L., & Croll, D. (2021). Rapid sequence evolution driven by transposable elements at a virulence locus in a fungal wheat pathogen. *BMC Genomics*, *22*(1), 1–16. https://doi.org/10.1186/s12864-021-07691-2

Sun, X., Ruan, R., Lin, L., Zhu, C., Zhang, T., Wang, M., Li, H., & Yu, D. (2013). Genomewide investigation into DNA elements and ABC transporters involved in imazalil resistance in penicillium digitatum. *FEMS Microbiology Letters*, *348*(1), 11–18. https://doi.org/10.1111/1574-6968.12235

Torriani, S. F. F., Melichar, J. P. E., Mills, C., Pain, N., Sierotzki, H., & Courbot, M. (2015). Zymoseptoria tritici: A major threat to wheat production, integrated approaches to control. *Fungal Genetics and Biology*, *79*, 8–12. https://doi.org/10.1016/j.fgb.2015.04.010

Vestergård, N. F., Jørgensen, L. N., Hellin, P., & Heick, T. M. (2023). Fungicide spraying intensity in the field drives the selection of amino acid alteration conferring resistance in Zymoseptoria tritici. *European Journal of Plant Pathology*, *2050*, 385–401. https://doi.org/10.1007/s10658-023-02671-6